Chemical dependence of second-order radiative contributions in the $K\beta$ x-ray spectra of vanadium and its compounds

Stjepko Fazinić* and Milko Jakšić
Rudjer Bošković Institute, Bijenička cesta 54, 10000 Zagreb, Croatia

Luka Mandić and Julijan Dobrinić
Faculty of Engineering, University of Rijeka, Rijeka, Croatia
(Received 21 July 2006; published 1 December 2006)

$K\beta$ x-ray spectra of metallic vanadium and its compounds (V_2O_3, VO_2, V_2O_5, VC, VN, VCl_2, NH_4VO_3, and $VOSO_4\times 5H_2O$) induced in thick targets by 3 MeV proton beams were measured by using wavelength dispersive (WD) x-ray spectrometer. In addition to the main $K\beta_{1,3}$ x-ray line, "satellites" or second order contributions like $K\beta'$, $K\beta''$, $K\beta'''$, and $K\beta_{2,5}$ were clearly resolved. Intensities and positions of these lines relative to the $K\beta_{1,3}$ x-ray line have been extracted by fitting the spectra and corrected for x-ray sample self-absorption. The influence of the oxidation states and vanadium-ligand bond distances in studied compounds on relative intensities and positions of $K\beta''$, $K\beta_{2,5}$, and $(K\beta''+K\beta_{2,5})$ x-ray lines (relative to $K\beta_{1,3}+K\beta'$) has been studied and discussed. The obtained results indicate that the strength of the $K\beta''$ and $K\beta_{2,5}$ transition probability per vanadium-ligand pair decreases exponentially with increasing vanadium-ligand distance, in agreement with the observation reported by Bergman *et al.* for $K\beta''$ relative intensity in a number of Mn oxide compounds [U. Bergmann, C. R. Horne, T. J. Collins, J. M. Workman, and S. P. Cramer, Chem. Phys. Letters **302**, 119 (1999)].

DOI: 10.1103/PhysRevA.74.062501 PACS number(s): 33.20.Rm, 36.20.Kd, 78.70.En, 82.80.Ej

I. INTRODUCTION

Accurate knowledge of $I(K\beta)/I(K\alpha)$ x-ray intensity ratios is of prime importance in applied and basic research, including elemental analysis by x-ray emission techniques and for studying physical processes in plasmas. Recently it has been proposed to use the $I(K\beta)/I(K\alpha)$ x-ray intensity ratios as a promising sensitive tool for studying quantitatively the changes of the valence electronic configurations of $3d$ transition metals in various compounds and alloys [1–7], based on the well known fact that the $I(K\beta)/I(K\alpha)$ x-ray intensity ratios in $3d$ elements depend on the chemical environment and the excitation mode.

The available literature contains a large volume of experimental data on the $I(K\beta)/I(K\alpha)$ x-ray intensity ratios in x-ray spectra emitted as a result of inner-shell ionization. Systematic discrepancy between experimental data and theoretical predictions for deexcitation of a single K vacancy in a neutral atom [8] has been observed in the atomic number region between $Z=21$ and $Z=32$, i.e., for transition metals where the $3d$ subshell is filling [9]. Various atomic models to obtain realistic wave functions and theoretical calculations for x-ray emission rates, and in the case of molecules and solids molecular orbital methods for electronic structures and molecular wave functions, have been recently reviewed by Mukoyama [10]. Most experimental studies on the chemical effect and the excitation mode dependence of $I(K\beta)/I(K\alpha)$ x-ray intensity ratios were performed with solid-state detectors (SSD). Owing to the poor energy resolution of SSD, the fine structures in $K\alpha$ and $K\beta$ lines cannot be resolved. This influences the reliability of most experimental data obtained by these detectors. In addition, most of the experimental data have been obtained by very rough methods of data analysis [9].

It is expected that $K\alpha$ spectra are not so sensitive to chemical effects since they are emitted through transition between inner shells. More pronounced chemical bond effects are expected to result from the $K\beta$ band, especially in the features that are connected to valence electrons. When measured with wavelength dispersive (WD) spectrometers, the structure of the $K\beta$ region shows one prominent x-ray line ($K\beta_{1,3}$) and several satellite lines or second order contributions. The literature contains a copious volume of experimental data on the fine structure of the $K\beta$ spectral region obtained by using the WD detector systems. Spectra of $3d$ elements and their compounds measured with such detectors may resolve the $K\beta$ spectral region to a number of components. In addition to the most intensive $K\beta_{1,3}$ x-ray line, satellites such as KMM and $K\beta'$ at the low energy side of the $K\beta_{1,3}$, and $K\beta''$, $K\beta_{2,5}$ and $K\beta'''$ at the high energy side of the $K\beta_{1,3}$, may be seen. Here KMM stands for radiatiave $K\rightarrow MM$ Auger transition, which is observed as a long tail with a maximum at about 100 eV below the $K\beta_{1,3}$ peak [11,12]. An explanation for $K\beta'$, located about 10–15 eV below the $K\beta_{1,3}$, is offered in terms of the electron interaction between the partially filled $3p$ and $3d$ subshells of the configuration representing the final state of the transition [13,14]. $K\beta'''$ represents the x-ray line that arise from the simultaneous creation of a K- and L-shell vacancy by incoming radiation, and in case of vanadium is located about 50–70 eV above the $K\beta_{1,3}$ x-ray line [15]. $K\beta''$ and $K\beta_{2,5}$ x-ray lines correspond to transitions from molecular orbitals (MO) to the $1s$ metal orbital, and for $3d$ elements and their compounds they are located in between $K\beta_{1,3}$ and $K\beta'''$ x-ray lines [16,17]. These transitions are obvious candidates for

*Author to whom correspondence should be addressed.

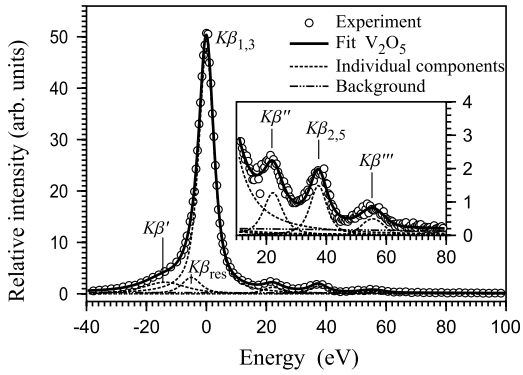

FIG. 1. Fitted V_2O_5 spectrum with indicated peak positions.

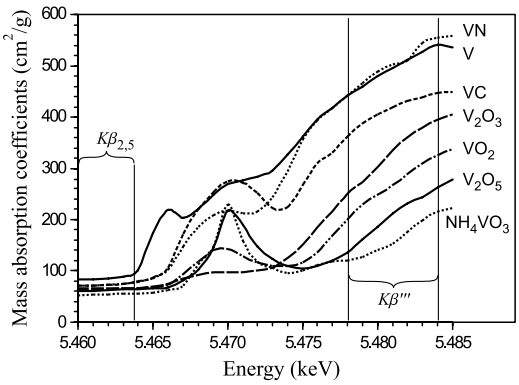

FIG. 2. The plots of absorption coefficients in the energy range between 5.46 to 5.485 keV for V metal and selected vanadium compounds, estimated from the corresponding normalized XANES spectra [35,37] and XCOM [31] results before and after the absorption edge.

chemically sensitive x-ray emission spectrometry, since the character of the valence orbitals changes the most between different chemical species.

Many experimental data related to the investigation of chemical effects on the $K\beta$ x-ray band exist for $3d$ transition metals and their compounds. A broad understanding of the processes involved in generating $K\beta$ structures is handicapped by the fragmentary nature of existing publications, and difficulties when one has to compare experimental results obtained by a wide variety of experimental analysis procedures and interpretations.

Recently Gamblin and Urch [18] and Peng *et al.* [19] made systematic analysis of chemical effects related to $K\beta'$ -$K\beta_{1,3}$ x-ray region in transition metal compounds. Gamblin and Urch [18] noted that x-ray emission spectroscopy based on the analysis of $K\beta'$ and $K\beta_{1,3}$ x-ray intensity ratios is ideally suited for investigating Cr and Mn compounds, while for lighter and heavier metals this method is not useful due to experimental difficulties (lighter elements) or unclear trends of intensity ratios versus oxidation states (heavier elements). Critical review of a possibility to use x-ray emission spectroscopy by using electron beam instruments to determine the valence states of first-row transition elements was recently published by Armstrong [20]. Sakurai and Eba reported about the use of relative intensities of manganese $K\beta'$ and $K\beta_{2,5}$ x-ray lines for chemical speciation [21] and determination of site occupancy of cations in spinel-type manganese oxides [22].

Bergmann *et al.* [23] measured $K\beta$ band high resolution spectra of a number of Mn compounds, with a focus on analysis of $K\beta''$ and $K\beta_{2,5}$ x-ray lines. They concluded that $K\beta''$ and $K\beta_{2,5}$ transitions may be a promising tool for structural characterization of transition-metal complexes. Inspired by their work, here we decided to investigate chemical dependence of the $K\beta$ band x-ray transition energies and intensities of vanadium compounds, with the focus on relative intensities and positions of $K\beta''$ and $K\beta_{2,5}$ x-ray lines. In order to resolve $K\beta$ spectra into components, we made our measurements by using WD spectrometer and analyzed measured spectra by using a least-squares fitting procedure. Available quantitative data related to $K\beta$ spectral band of vanadium and its compounds are scarce and scattered in literature. Most quantitative data related to individual peak intensities published in the existing literature are directly extracted data from measured spectra, i.e., summed channel contents or even only centroid peak heights have been reported. Since weak $K\beta''$ and $K\beta_{2,5}$ x-ray lines are positioned on the high energy shoulder of much stronger $K\beta_{1,3}$ peak, reliability of such data is questionable. Another difficulty is related to the fact that almost all published data found in the available literature were obtained by using thick targets. Various attempts have been applied in the past in order to estimate the influence of x-ray self-absorption within targets to relative peak intensities. Since we also made our measurements on thick targets, we investigated both influences of the target self-attenuation correction and chemical effects to measured x-ray intensities. In order to estimate the influence of target self-attenuation we have used published data from the available literature on the near-K-edge absorption features for vanadium and its selected compounds, obtained by measurements on synchrotron x-ray sources.

II. EXPERIMENTAL AND DATA ANALYSIS

Measurements were performed at the Rudjer Bošković EN Tandem VDG Accelerator with 3 MeV proton beam. Beam currents of about 20 nA were applied. Simple experimental setup was used with samples positioned in a vacuum scattering chamber. X-rays from a sample exit from the vacuum chamber through 50 μm thin kapton foil into the high resolution spectrometer positioned at the 90° angle in respect to the beam direction. X-ray spectrometer is enclosed in helium atmosphere and consists of a LiF(110) flat analyzing crystal and a position sensitive proportional counter (PSPC). Details of the experimental setup may be found elsewhere [24,25]. Beam to target normal and detector to target normal of 45° were used. On the way from the sample to the PSPC, x-rays pass through the above mentioned kapton foil and follow a 30 cm long path to the analyzing crystal and another 30 cm to the PSPC through the helium at the atmospheric pressure, before entering into the counter through the 6.5 μm thick aluminized Mylar foil. Electronic signals from the detector were processed by the CANBERRA 2020 amplifiers, CANBERRA 8075 ADC modules and in house developed data acquisition and analysis system

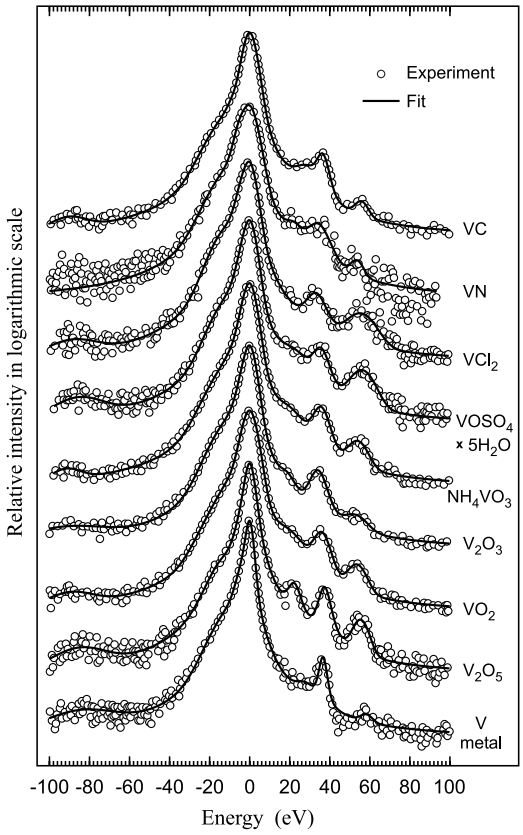

FIG. 3. Measured spectra of vanadium and its selected compounds. All the spectra are aligned relative to the centroid energy position of the $K\beta_{1,3}$ x-ray line.

SPECTOR [26]. The resolution of the detector system is mainly defined by the width of the proton beam on a target. With the effective slit width of 2 mm and the operating distance of 60 cm between the target and the PSPC detector, a resolution of 5.3 eV (FWHM) has been achieved for the $K\beta_{1,3}$ peak corresponding to the vanadium metal sample.

Vanadium compounds V_2O_3, VO_2, V_2O_5, VC, VN, VCl_2, NH_4VO_3, and $VOSO_4 \times 5H_2O$ were high purity powders obtained from Aldrich Chemical and Kemika Ltd. Actual measurement samples were mixed with graphite powder to avoid sample charging, and pressed into about 1 mm thick disks with 10 mm diameter. Spectra of elemental vanadium were also measured by using thick vanadium metallic foil.

In the data analysis, we first performed a least-χ-square fit of the spectra by using the wxEWA (V0.29a-Alpha8) least squares fitting program [27]. Pseudo-Voigt functions were used to describe $K\beta_{1,3}$, $K\beta'$, $K\beta''$, and $K\beta_{2,5}$ x-ray lines. All the fitting parameters were kept free except Gaussian-Lorenztian mixing that was linked to the highest peak ($K\beta_{1,3}$). In analysis of the $K\beta'$-$K\beta_{1,3}$ region we followed a procedure similar to the one used by Gamblin and Urch [18], i.e., we introduced additional residual pseudo-Voigt line $K\beta_{res}$ positioned in between that of $K\beta'$ and $K\beta_{1,3}$ x-ray lines. The Gaussian function was used for the $K\beta'''$ ($K\beta L^1$) and for the KMM contributions. A linear function with a negative slope was used for the background description. Energy calibration was established by using spectra obtained from metallic vanadium sample, based on the reported energies for $K\beta_{1,3}$ and $K\beta_{2,5}$ x-ray lines from Bearden [28], i.e., 5427.32 eV for $K\beta_{1,3}$ line, and 5462.96 eV for $K\beta_{2,5}$ line. Figure 1 shows the spectrum of V_2O_5 fitted by the model explained, with indicated peak positions.

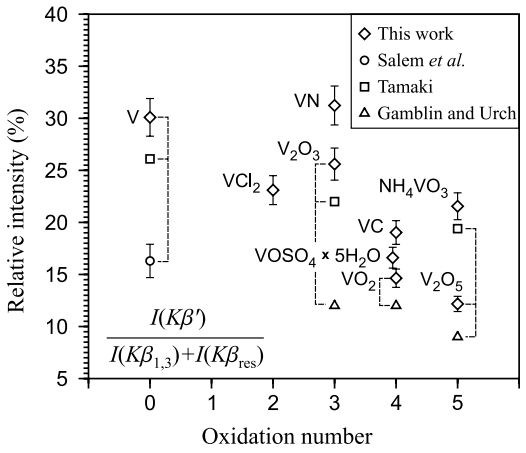

FIG. 4. Measured intensities of $K\beta'$ relative to $K\beta_{1,3}$ x-ray line for all the samples. Residual peak $K\beta_{res}$ is included in $K\beta_{1,3}$. Results published by Salem *et al.* [48], Tamaki [49], and Gamblin and Urch [18] are also presented.

Peak intensities obtained from the fitted spectra were then corrected for the sample self-absorption. It is important to study the amount of this correction since the K-shell absorption edge is situated slightly above the $K\beta_{1,3}$ region. This correction is negligible when studying intensity ratios of $K\beta'$ to $K\beta_{1,3}$, but may be of importance when studying intensity ratios of $K\beta''$, $K\beta_{2,5}$, and $K\beta'''$ to $K\beta_{1,3}$.

From the available literature we could see that most results on $K\beta$ x-ray relative intensities published so far were obtained by analysis of thick targets. In some cases reported results were not corrected for the sample self-attenuation. In other cases the influence of the sample self-attenuation was estimated in different ways. Any such correction relay on the

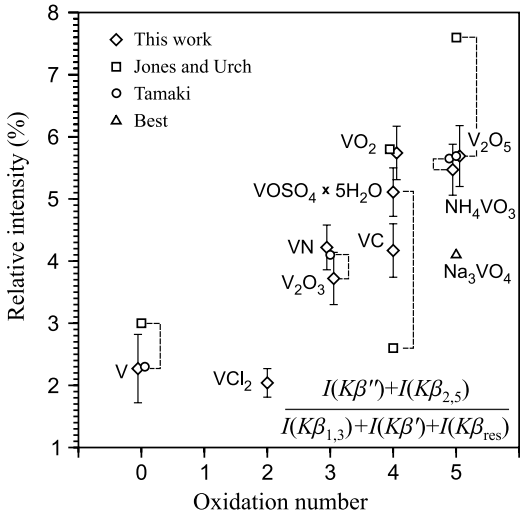

FIG. 5. Intensities of $(K\beta''+K\beta_{2,5})$ relative to $(K\beta_{1,3}+K\beta')$ for all the samples. Residual peak $K\beta_{res}$ is included in $K\beta_{1,3}$. Results published by Jones and Urch [54], Tamaki [49], and Best [68] are also presented.

TABLE I. Measured intensities of $K\beta''$, $K\beta_{2,5}$, and their sum $(K\beta''+K\beta_{2,5})$, relative to $(K\beta_{1,3}+K\beta'+K\beta_{res})$ intensities in percent and their comparison with other experimental results from the literature.

Sample	$K\beta''$	$K\beta_{2,5}$	$(K\beta''+K\beta_{2,5})$	Reference
V	0.81±0.14	1.46±0.45	2.27±0.55	This work
		2.52		Török *et al.* [77]
		4.6		Asada *et al.* [53]
	-	3	3	Jones and Urch[54]
	0.48	1.82	2.3	Tamaki[49]
VCl_2		2.04±0.23	2.04±0.23	This work
V_2O_3	1.02±0.13	2.70±0.28	3.72±0.42	This work
		4.56		Asada *et al.* [53]
	1.64	2.46	4.1	Tamaki [49]
VN	1.29±0.22	2.93±0.28	4.22±0.36	This work
VO_2	3.07±0.32	2.67±0.28	5.74±0.43	This work
	3.2	2.6	5.8	Jones and Urch [54]
		5		Asada *et al.* [53]
VC	2.29±0.25	1.88±0.35	4.17±0.43	This work
V_2O_5	2.76±0.34	2.93±0.35	5.69±0.49	This work
		5.5		Asada *et al.* [53]
	4	3.6	7.6	Jones and Urch [54]
	3.18	2.51	5.69	Tamaki [49]
NH_4VO_3	2.89±0.31	2.58±0.27	5.47±0.41	This work
	3.8	3.4	7.2	Jones and Urch [54]
	3.11	2.54	5.65	Tamaki [49]
$VOSO_4\times 5H_2O$	2.94±0.33	2.17±0.21	5.11±0.39	This work
	1	1.6	2.6	Jones and Urch [54]
Na_3VO_4	2.2	1.9	4.1	Best [68]

knowledge of absorption coefficients close to the *K*-shell absorption edge. Usual sources of these coefficients are standard tables, such as those of McMaster *et al.* [29], Thinh and Leroux [30], XCOM [31], and others [32]. It is well known that these tables do not provide very accurate data about absorption coefficients close to the absorption edges. For example, when using XCOM data for absorption coefficients, the sharp step corresponding to the vanadium *K*-shell absorption edge is located at the energy of 5465 eV, which is very close to reported energies of $K\beta_{2,5}$ x-ray line. Therefore, we studied available data about x-ray emission and absorption bands (and related absorption coefficients) close to the vanadium *K*-shell absorption edge. Some qualitative results of near the *K*-edge band structure may be found in older Refs. [33,34]. We decided to use more reliable quantitative data found in several recent papers focused on x-ray-absorption near-edge structure (XANES) analysis of vanadium compounds. We estimated respective x-ray absorption coefficients close to the vanadium *K*-edge by using normalized absorption spectra of V_2O_3, VO_2, and V_2O_5 published by Dubiel *et al.* [35], and normalized absorption spectra of V, VC, VN, and NH_4VO_3, published by Wong *et al.* [36], in connection with the XCOM results [31] for absorption coefficients before and after the absorption edge. The plots of absorption coefficients obtained in such a way in the energy range between 5.46 to 5.485 keV for vanadium metal and the above mentioned vanadium compounds is presented in Fig. 2.

In order to calculate self-absorption correction from thick samples, the existing TTPIXAN code [37] was modified to allow the use of the above absorption coefficients instead of those normally used [30] by the program. This code calculates x-ray yields from thick targets as the integral of x-ray intensities reaching an x-ray detector from successive points along proton trajectories in the target. Actually, integration is replaced by the summation of x-ray yields emerging from a number of thin slices. By using energy loss data the program calculates proton energies in each thin slice within the sample. X-ray yields from each slice are calculated by using the corresponding *K*-shell ionization and x-ray production cross sections, and by taking in account self-attenuation of x-rays within the sample on their way to the detector. This is a standard procedure for calculating thick target x-ray yields used by particle induced x-ray emission (PIXE) analysis program packages [38]. In calculation of x-ray yields the TTPIXAN code employs proton stopping powers of Janni [39] and perturbed-stationary-state (PSS) theory with energy-loss (E), Coulomb defection (C), and relativistic (R) corrections (ECPSSR) x-ray ionization cross sections [40,41] calculated by using the approach given by Cohen [42], Benka's tables [43] of universal function, and Paul's correction factors [44]. Since 3 MeV protons have different energy loss

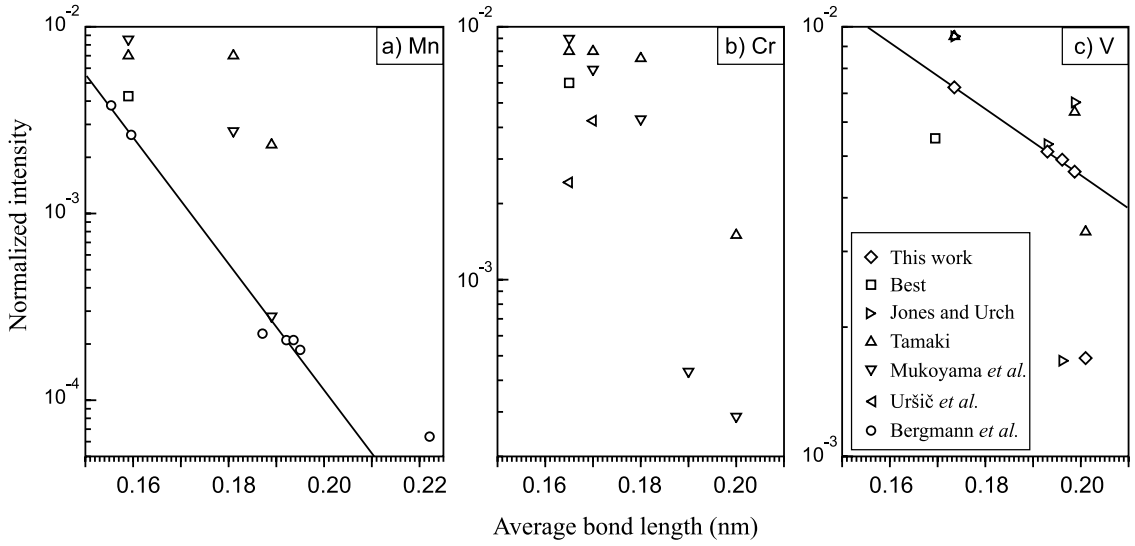

FIG. 6. Intensities of $K\beta''$ x-ray line relative to the $(K\beta_{1,3}+K\beta'+K\beta_{res})$ intensities and divided by the number of oxygen ligands per central metal ion, as a function of the average metal-oxygen distance, for Mn (a), Cr (b), and V (c) oxide compounds. In addition to our measured data, experimental data of Best [68], Jones and Urch [54], Tamaki [49], Uršič *et al.* [47], and Bergmann *et al.* [23], together with theoretical results of Mukoyama *et al.* [56] are presented.

and range in each of the targets used in this work, and since *K*-shell ionization cross sections (and corresponding x-ray production cross sections) are energy dependent, the depth profile of detected x rays is different for each of the measured targets. As example, the range of 3 MeV protons in measured samples varies for about 40 μm. This has an influence on detected x-ray intensity ratios, i.e., the ratios measured by using thick targets are different from those measured on thin targets. Thick target yields obtained by TTPIXAN have been used to calculate theoretical thick target $K\beta'/K\beta_{1,3}$, $K\beta''/K\beta_{1,3}$, $K\beta_{2,5}/K\beta_{1,3}$, and $K\beta'''/K\beta_{1,3}$ intensity ratios. Results of such calculations have been used to calculate the self-absorption correction factors, i.e., thick-to-thin target intensity ratios. Thin target intensity ratios are generally more relevant for studying possible chemical dependence of second order radiative contributions in the $K\beta$ x-ray spectra then the related thick target ratios.

As, expected, the analysis has shown that the self-absorption correction factors are: (i) negligible in the case of $K\beta'/K\beta_{1,3}$ and $K\beta''/K\beta_{1,3}$ intensity ratios; (ii) small (between 1.009 and 1.07) for $K\beta_{2,5}/K\beta_{1,3}$ intensity ratios; (iii) high (for vanadium metal 4.8, and for studied vanadium compounds between 1.3 and 3.7) for $K\beta'''/K\beta_{1,3}$ intensity ratios. In practice it means that intensity ratios obtained by using thick targets, as compared to thin target ratios are: (i) the same for $K\beta'/K\beta_{1,3}$ and $K\beta''/K\beta_{1,3}$; (ii) slightly smaller (from 1 to 7%) for $K\beta_{2,5}/K\beta_{1,3}$, and (iii) much smaller for $K\beta'''/K\beta_{1,3}$.

The corresponding uncertainties in $K\beta_{2,5}/K\beta_{1,3}$ intensity ratios are estimated to less than 10% for vanadium compounds and to about 30% for vanadium metal (mainly due to a prepeak in the normalized absorption coefficient, which is positioned very close to the energy position of the $K\beta_{2,5}$ line).

As the results of the analysis show, in case of thick targets, $K\beta'''/K\beta_{1,3}$ intensity ratios are highly influenced by the strong $K\beta'''$ self-absorption in samples. The situation in calculating thick-to-thin target correction factor for $K\beta'''/K\beta_{1,3}$ intensity ratios is further complicated since the intensity of the $K\beta'''$ multiple vacancy satellite depends on the ratio of double to single ionization cross section, which is also energy dependent. This means that the x-ray production cross section for $K\beta'''$ line in different depths in the target has different profile then the one related to the $K\beta_{1,3}$ line. In calculating $K\beta'''$ thick target yields we have used Cue *et al.* [45] data about the ratio of the vanadium double to single ionization cross sections. In addition, $K\beta'''$ line is very close to the *K* edge and related absorption coefficients for this line are much higher then for the other x-ray lines measured. The uncertainties of reported $K\beta'''/K\beta_{1,3}$ intensity ratios due to absorption coefficients are estimated to 20%, except in the case of V_2O_5, where this error is estimated to 35%.

In calculation of the x-ray self-absorption corrections we took in to account the fact that actual samples were mixtures of vanadium compounds and graphite powder. All the correction factors given here are for actually used samples.

In addition, corrections related to the detector efficiency and crystal reflectivity, as well as to the absorption of x-rays in kapton, aluminized Mylar foil, and helium gas were done. Altogether combining the level of these corrections was between 0.2–2.2%.

III. RESULTS AND DISCUSSION

Our work has been focused to the analysis of $K\beta''$ and $K\beta_{2,5}$ x-ray lines and most of the discussion in this paper will be related to relative positions and intensities of these two lines in respect to the low energy region of the $K\beta$ x-ray band. Reported intensities of $K\beta''$ and $K\beta_{2,5}$ presented in this paper are normalized to the sum of $(K\beta_{1,3}+K\beta'+K\beta_{res})$ intensities, and their positions are relative to the fitted position of the $K\beta_{1,3}$ peak centroid.

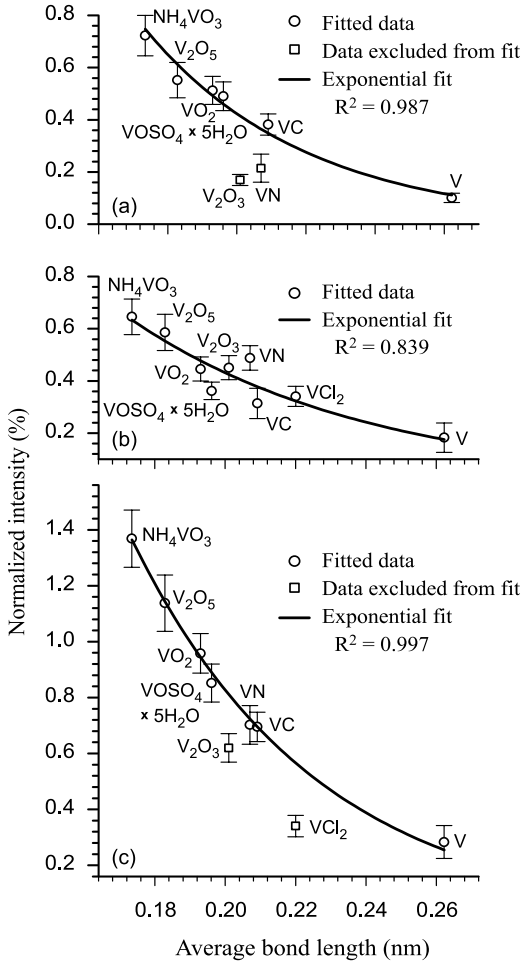

FIG. 7. Relative intensities of $K\beta''$ (a), $K\beta_{2,5}$ (b), and $(K\beta''+K\beta_{2,5})$ (c), normalized to the intensity of $(K\beta_{1,3}+K\beta'+K\beta_{res})$ and divided by the number of ligands per the central vanadium ion (i.e., number of vanadium-ligand pairs), as a function of the average vanadium-ligand distance.

Figure 3 shows all the measured spectra. To address relative positions of the peaks, the spectra were processed by aligning them to the position of the $K\beta_{1,3}$ line and setting its relative energy to zero.

A. $K\beta'$ x-ray line

Before presenting and discussing our results related to $K\beta''$ and $K\beta_{2,5}$ x-ray lines, a brief discussion about the analysis of the $K\beta'-K\beta_{1,3}$ region will be given.

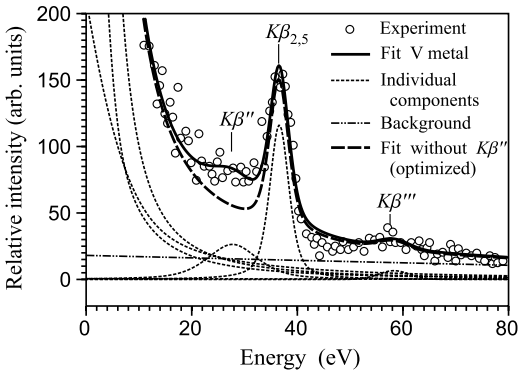

FIG. 8. Higher energy portion of the vanadium metal spectrum, showing experimental data, individual fitted lines, and the fit of the spectrum with and without the $K\beta''$ x-ray line.

Analysis of $3d$ elements' $K\beta'$-$K\beta_{1,3}$ structure and processes involved has been the subject of research for a long time. According to the simple model developed by Tsutsumi [13,14], the origin of $K\beta'$ peak is ascribed to consumption of part of the $K\beta_{1,3}$ energy in promoting an unpaired electron into an excited state, while relative intensity of the $K\beta'$ peak (in respect to $K\beta_{1,3}$) is proportional to the number of unpaired $3d$ electrons in compounds. Quantitative agreement between this simple model and experiment is not so good. Experimental data are scattered and difficult to compare due to variations in methods used for spectral analysis. With typical detectors these peaks are strongly overlapped and as shown by theoretical calculations [19] $K\beta'$-$K\beta_{1,3}$ structure consists of more than two closely positioned peaks. A majority of older and even recent papers report measured integrated intensities of $K\beta'$ relative to $K\beta_{1,3}$ (without fitting the measured spectra).

The most comprehensive study of recent years is that of Gamblin and Urch [18], and as we already explained, in the analysis of the $K\beta'$-$K\beta_{1,3}$ region we followed a procedure similar to the one used by them. They recorded over 60 different compounds of Ti, V, Cr, Mn, Fe, and Co, and analyzed the $K\beta'$-$K\beta_{1,3}$ region by fitting their spectra with three symmetric Voigt functions. During the fitting process, two extreme peaks ($K\beta'$ and $K\beta_{1,3}$) were made as intense as possible, and the third residual peak $K\beta_{res}$ positioned in between $K\beta'$ and $K\beta_{1,3}$ x-ray lines, was made sufficiently intense to fill any gap, and was considered to have a profile very similar to its stronger neighbors. However, since we measured our spectra with the intention to cover a wider energy, spanning the full $K\beta$ x-ray band, our spectra have been fitted with additional peaks, corresponding in the low

TABLE II. Measured $\Delta E(K\beta''-K\beta_{1,3})$ and $\Delta E(K\beta_{2,5}-K\beta_{1,3})$ in eV.

	V	VCl_2	V_2O_3	VN	VO_2	VC	V_2O_5	NH_4VO_3	$VOSO_4$ $\times 5H_2O$
ΔE(eV)	27.0	-	17.9	20.8	18.9	27.1	21.6	18.8	20.9
$(K\beta''-K\beta_{1,3})$	±0.3		±0.3	±0.3	±0.3	±0.3	±0.3	±0.3	±0.3
ΔE(eV)	35.6	31.8	32.7	32.7	34.5	35.0	36.4	34.2	34.6
$(K\beta_{2,5}-K\beta_{1,3})$	±0.3	±0.4	±0.4	±0.5	±0.4	±0.4	±0.4	±0.4	±0.4

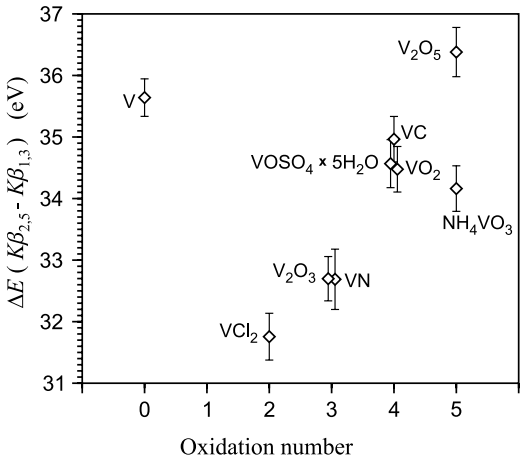

FIG. 9. Measured energy of the $K\beta_{2,5}$ x-ray line relative to the position of the $K\beta_{1,3}$ peak for all the measured samples.

energy part to the radiative Auger (KMM), and at the higher energy side to $K\beta''$, $K\beta_{2,5}$, and $K\beta'''$ x-ray lines. In their analysis, Gamblin and Urch [18] added the $K\beta_{res}$ peak inspired by the work of Peng *et al.* [19], who measured highly resolved $K\beta$ x-ray emission spectra for a number of Mn(II), Mn(III), and Mn(IV) compounds and calculated their theoretical spectra by using the ligand field atomic multiplet model [46]. Contrary to this approach, Uršič *et al.* [47] used just two pseudo-Voigt peaks to fit $K\beta'$-$K\beta_{1,3}$ structure for several Cr compounds, and Salem *et al.* [48] used three Gaussian peaks, named $K\beta'$, $K\beta_1$, and $K\beta_3$, all three with the same FWHM, with $K\beta_3$ positioned in between the $K\beta'$ and $K\beta_1$, with its centroid height being one half of the $K\beta_1$ height (inspired probably by the Scofiled's HFS calculations for free atom [8]). In his report Tamaki [49] used hyperbolic functions to represent individual peaks (one for $K\beta'$ and one for $K\beta_{1,3}$, without introducing residual third peak in between).

Figure 4 presents our results for $I(K\beta')/I(K\beta_{1,3})$ intensity ratios, together with previously published results related to vanadium and its compounds as reported by Salem *et al.* [48], Tamaki [49], and Gamblin and Urch [18].

Peng *et al.* [19] found that $K\beta'$ feature is weaker and broader for higher oxidation states, and almost unobservable for low-spin Mn(III). They observed that strong final-state $3p3d$ exchange coupling results in a sensitivity of $K\beta'$ intensity to $3d$ population and to the relative spin orientation of $3p$ and $3d$ electrons. Other authors [18,22,49] reported that relative $K\beta'$ intensities decrease with increasing oxidation number for a range of transition metal compounds. Our results for selected vanadium compounds are in qualitative agreement with these observations.

Ekstig *et al.* [50] and Salem *et al.* [48] reported higher measured relative intensities of $K\beta'$ x-ray line for investigated metal oxides when compared with spectra of related metals. Theoretical values derived on the basis of a simple exchange interaction predict the opposite trend [48]. Uršič *et al.* [47] investigated $K\beta'$ intensity for Cr and several Cr oxides, and reported that $K\beta'$ relative intensity in investigated oxides was lower than in the pure metal, which agrees with results of Tamaki [49] and our observations for vanadium and related oxides (Fig. 4).

B. $K\beta''$ and $K\beta_{2,5}$ x-ray lines

Experimental data related to intensities of $K\beta''$ and $K\beta_{2,5}$ are often plotted against the formal oxidation number of metals. It was qualitatively shown for a range of Ti, Cr, Mn, and Fe oxide compounds [16,51,52] that the $K\beta''$ intensity increases with an increase in the oxidation number of a transition metal atom. Asada *et al.* [53] measured $K\beta_{2,5}$ intensities for a range of oxide compounds of $3d$ transition metals, including vanadium and VO, V_2O_3, V_2O_4, and V_2O_5. Simple peak intensity ratios of $K\beta_{2,5}/K\beta_{1,3}$ extracted from the measured spectra without fitting were reported to vary from 4.56% to 5.5% with an increasing oxidation number from 2 to 5. Jones and Urch [54] reported relative intensity ratios of $K\beta''$ and $K\beta_{2,5}$ x-ray lines from the metal, VO_2, V_2O_5, $VOSO_4 \times 5H_2O$, NH_4VO_3, and $NH_4V_3O_8$. In fact, instead of peak relative intensities, they reported measured peak heights. Tamaki [49] reported relative intensity ratios of vanadium $K\beta''$ and $K\beta_{2,5}$ x-ray lines from the metal vanadium, V_2O_3, V_2O_5, and NH_4VO_3, based on fitting the spectra by hyperbolic functions. Table I shows our results for $K\beta''$ and $K\beta_{2,5}$ relative intensities, together with the results published by others. The table also gives relative intensities of the sum of $K\beta''$ and $K\beta_{2,5}$ x-ray lines. Qualitatively, relative intensities of both lines increase with an oxidation number. This is better seen for $(K\beta''+K\beta_{2,5})$ relative intensities (Fig. 5). However, as already pointed out by Mukoyama [1], the oxidation number is not a good quantitative measure and can be used only for qualitative discussions because it is defined as an integer and different x-ray intensity ratios are observed for compounds with the same oxidation number.

Möser [55] and Mukoyama [1] investigated the dependence of $K\beta/K\alpha$ ratios as a function of bond length. Bergmann *et al.* [23] measured $K\beta$ band high resolution spectra of a number of Mn compounds, with a focus on analysis of $K\beta''$ and $K\beta_{2,5}$ x-ray lines. They found that for oxygen-ligated Mn compounds the measured strength of the $K\beta''$ transition decreases exponentially with increasing average Mn-O bond distance. They claim that in such a way it is possible to predict average bond distances in Mn oxide compounds to $\approx$0.01 nm. They concluded that $K\beta''$ and $K\beta_{2,5}$ transitions may be a promising tool for structural characterization of transition-metal complexes and, since $K\beta''$ energy is related to the ligand $2s$ binding energy, it can be used to identify the type of ligand in Mn compound.

Figure 6 shows intensities of $K\beta''$ x-ray line relative to the $(K\beta_{1,3}+K\beta'+K\beta_{res})$ intensity and divided by the number of oxygen ligands per central metal ion, as a function of the average metal-oxygen distance, as compiled from the available literature data for a number of various Mn, Cr, and V oxide compounds [Figs. 6(a)–6(c)]. The solid line in Fig. 6(a) is the least-squares fit (using exponential function) through the data published by Bergmann *et al.* [23] prepared in the same way as they did in their paper. The figure also shows theoretical results for several Mn and Cr oxide compounds of tetrahedral and octahedral symmetries, as obtained by Mukoyama *et al.* [56] by using the discrete variational (DV) $X\alpha$ MO cluster method. According to their calculations, for oxide compounds with tetrahedral symmetry, intensities of $K\beta''$ and $K\beta_{2,5}$ satellite lines increase $K\beta/K\alpha$ inten-

TABLE III. Available experimental literature data for the energy difference between $K\beta_{2,5}$ and $K\beta''$ x-ray lines for various $3d$ metal compounds with four different ligands (carbon, nitrogen, oxygen, and fluorine).

	$\Delta E(K\beta_{2,5}-K\beta'')$ (eV)				
Compound	Carbon	Nitrogen	Oxygen	Fluorine	Reference
VC	7.9				This work
	6.5				Gubanov [73]
	7.1				Sheludchenko [74]
$VC_{0.88}$	7				Ramquist *et al.* [78]
$VC_{0.72}$	7				Ramquist *et al.* [78]
VN		11.9			This work
		13			Gubanov [73]
		11.1			Sheludchenko [74]
		12.2			Romand *et al.* [79]
$VN_{0.82}$		12.2			Romand *et al.* [79]
VO			14.7		Gubanov [73]
V_2O_3			14.8		This work
VO_2			15.5		This work
V_2O_5			14.8		This work
			14.8		Jones and Urch [54]
NH_4VO_3			15.4		This work
			15.1		Jones and Urch [54]
$NH_4V_3O_8$			15.1		Jones and Urch [54]
$VOSO_4\times 5H_2O$			13.6		This work
			12.1		Jones and Urch [54]
Na_3VO_4			14.6		Best [68]
Sc_2O_3			15.1		Kawai *et al.* [69]
ScF_3				19.8	Kawai *et al.* [69]
TiC	7				Blokhin and Shuaev [80]
	7				Vainshtein *et al.* [81]
TiN		10			Blokhin and Shuaev [80]
		11.3			Vainshtein *et al.* [81]
TiO			15.7		Ern and Switendick [82]
TiO_2			15.6		Dräger *et al.* [83]
			15.2		Koster and Mendel [16]
Na_2TiF_6				20	Koster and Mendel [17]
Cr_2O_3			13.9		Koster and Mendel [16]
CrO_3			15.5		Koster and Mendel [16]
K_2CrO_4			15.9		Best [68]
			16.5		Uršič *et al.* [47]
$K_2Cr_2O_7$			16		Uršič *et al.* [47]
Mn(salen)N		10.3			Bergmann *et al.* [23]
MnO			15.2		Tsutsumi *et al.* [14]
			15		Bergmann *et al.* [23]
MnO_2			13.7		Koster and Mendel [16]
			14.6		Sakurai and Eba [21]
			14.2		Sakurai and Eba [22]
			16.1		Tsutsumi *et al.* [14]
Mn_2O_3			15.1		Sakurai and Eba [22]
Mn_3O_4			15		Sakurai and Eba [21]
			15.4		Sakurai and Eba [22]

TABLE III. (*Continued.*)

Compound	$\Delta E(K\beta_{2,5}-K\beta'')$ (eV) Carbon	Nitrogen	Oxygen	Fluorine	Reference
MnO_4^-			14.5		Koster and Mendel [16]
$KMnO_4$			15.5		Bergmann *et al.* [23]
			14.8		Tsutsumi *et al.* [14]
			14.4		Best [68]
			13.8		Sakurai and Eba [21]
K_2MnO_4			16		Tsutsumi *et al.* [14]
$LiMn_2O_4$			15.4		Sakurai and Eba [22]
$Ba_3\ (MnO4)_2$			15		Sakurai and Eba [21]
$ZnMn_2O_4$			14.9		Bergmann *et al.* [23]
$MnCo_2O_4$			15.4		Sakurai and Eba [22]
MnF_2				20	Bergmann *et al.* [23]
K_3MnF_6				19.7	Koster and Mendel [17]
K_2MnF_6				19.6	Koster and Mendel [17]
energy range (eV)	⟨5.9–7.9⟩	⟨9.3–13⟩	⟨13.6–16.5⟩[a]	⟨19.6–20⟩	

[a]With the exception of the value of 12.1 for $VOSO_4\times 5H_2O$ reported by Jones and Urch [54].

sity ratios considerably, while in octahedral symmetry their contribution to total $K\beta$ intensity is much smaller. Figure 6 shows that data from different sources are scattered and difficult to compare. However, the results obtained by Bergmann *et al.* [23] for $K\beta''$ on Mn oxide-compounds inspired us to investigate similar dependence of $K\beta''$, $K\beta_{2,5}$, and $(K\beta''+K\beta_{2,5})$ normalized intensities for various vanadium compounds. Corresponding results for vanadium oxide compounds are included in Fig. 6(c), together with other data from the literature, and with the exponential fit line through our data.

In preparation of Fig. 6 we have used metal-ligand bond distances as found in the available literature. These distances, together with some other basic data about studied vanadium compounds are given below.

V_2O_3 (oxidation number 3) has a corundum structure in which V^{3+} ions are sixfold coordinated by oxygen ions at two distinct distances, 0.196 and 0.206 nm [57]. The average bond distance is 0.201 nm. The site symmetry of the vanadium atom is C_3.

The crystal structure of VO_2 (oxidation number 4) is monoclinic and is a distorted form of rutile [58,59]. The site symmetry of the vanadium atom is C_1. In VO_2 the vanadium atoms are sixfold coordinated by oxygen ions, but are much displaced from the center of the octahedron, resulting in one short V-O bond of length 0.176 nm. The other bond distances are 0.186, 0.187, 0.201, 0.203, and 0.205 nm, resulting with the average bond length of 0.193 nm.

According to Bachmann *et al.* [60], in V_2O_5 (oxidation number 5), vanadium is fivefold coordinated in a distorted tetragonal pyramid of oxygen. The apex-oxygen distance is only 0.1585 nm, whereas the basal V-O distances are 0.178, 0.1878, 0.1878, and 0.2021 nm, resulting with the average bond distance of 0.183 nm. However, there is a sixth oxygen from a VO_5 unit below the vanadium, which is too far to be considered in the primary coordination sphere, at the distance of 0.278 nm. With this oxygen included, the resulting average bond distance would be 0.199 nm. The site symmetry of the vanadium atom is C_s. Enjalbert and Galy [61] reported the same bond distances, with the comment that V_2O_5 has a layered structure built up from VO_5 square pyramids sharing edges and corners, with V_2O_5 sheets held together via weak vanadium-oxygen interlayer interaction (with 0.279 nm bond distance) that cannot be treated as a real bond.

NH_4VO_3 (oxidation number 5) structure consists of tetrahedral VO_4 chains with two types of V-O bonds [62]. Within the VO_4 tetrahedron two bonds are formed with oxygen atoms which link the tetrahedra together and have a V-O dis-

TABLE IV. Relative intensities $I(K\beta''')/I(K\beta_{1,3}+K\beta'+K\beta_{res})$ in percent and $\Delta E(K\beta'''-K\beta_{1,3})$ in eV.

	V	VCl_2	V_2O_3	VN	VO_2	VC	V_2O_5	NH_4VO_3	$VOSO_4\times 5H_2O$
Relative	0.5	1.3[a]	0.8	1.0	1.3	0.8	1.7	0.9	1.5*
intensity	±0.2	±0.3	±0.2	±0.3	±0.3	±0.2	±0.6	±0.2	±0.3
ΔE (eV)	56.8	53.4	50.8	51.4	51.4	53.5	54.0	51.8	54.8
	±1.0	±0.7	±0.6	±1.3	±0.6	±0.6	±0.6	±0.6	±0.6

[a]No correction for self-attenuation.

tance of 0.181 nm. The other two bonds are formed with terminal (unlinked) oxygens in the mirror plane and have a shorter V-O distance of 0.166 nm. The average bond distance is 0.174 nm.

VC (oxidation number 4) [63] and VN (oxidation number 3) [64] are intermetallic compounds with the same NaCl type lattice where vanadium atoms are octahedrally coordinated by the atoms of the ligand sublattice. Bond distance is 0.209 nm for VC, and 0.207 nm for VN.

The crystal structure of $VOSO_4 \times 5H_2O$ is monoclinic [65]. The structure consists of molecular units built up of a SO_4 tetrahedron and a VO_6 octahedron sharing one apex. Four water molecules are coordinated with the vanadium. Four equatorial V-O bond distances are about 0.2 nm. One of the two axial V-O bond distances relate to short vanadyl oxygen at 0.1584 nm while the other bond length is 0.2181 nm. The average bond distance is 0.1965 nm.

VCl_2 (oxidation number 2) is a saltlike solid with polymeric structure. It has octahedral coordination geometry. Bond distances data are not so reliable [66] and are estimated to about 0.22 nm [67].

Figures 7(a)–7(c) show our results for all the measured samples and for normalized intensities of $K\beta''$, $K\beta_{2,5}$ and their sum, divided by the number of vanadium-ligand bonds per central metal ion. Exponential function $I_n = ae^{-bd}$ (I_n being the normalized intensity, d is the average bond length, while a and b are fit parameters) has been fitted through the experimental data to guide the eye.

Fitted line at Fig. 7(a) indicates exponential relationship between $K\beta''$ normalized intensities and average bond distances for measured compounds and the vanadium metal. V_2O_3 and VN have been excluded from the fit as outliers. Especially V_2O_3 show much smaller normalized $K\beta''$ intensity then the fitted line would suggest. Table II shows that V_2O_3 has the smallest energy difference between $K\beta''$ and $K\beta_{1,3}$ peaks. Taking in to account how close these lines are, one possible explanation for such a small V_2O_3 $K\beta''$ relative intensity could be that in this respect the analysis of V_2O_3 spectra failed, i.e., that one portion of the $K\beta''$ intensity has been assigned to the $K\beta_{1,3}$ x-ray line. Further measurement with a detection system having better energy resolution may help to resolve this issue and clarify a possibility if some other (physical) reason is responsible for the observed deviation. $K\beta''$ x-ray line was not observed in the case of VCl_2.

According to Best [68], $K\beta''$ x-ray line does not appear in the metal spectra, i.e., in the absence of the oxygen atoms. At the other hand, Kawai *et al.* [69] reported a strong $K\beta''$ x-ray line in Sc metal. They assigned this line to the hole transition from $1s^{-1}$ to an antibonding molecular orbital which is formed between center Sc $3p$ and surrounding Sc $3p$ orbitals. Figure 8 shows our recorded vanadium spectrum. Although the peak that could correspond to $K\beta''$ is not directly resolved in the spectrum, the spectrum cannot be properly fitted without an introduction of a peak at the position which is slightly below the $K\beta_{2,5}$ peak. In line with the assumption of Kawai for scandium metal spectra, we assumed that this is $K\beta''$ peak and its intensity given in Table I divided by 8 (corresponding to 8 V-V bonds [70]) is shown at Fig. 7(a).

Jones and Urch [54] and Best [68] have assigned $K\beta''$ peaks observed in transition-metal oxides as ligand $2s$ to metal $1s$ "interatomic" or "crossover" transitions, with the argument that the intensity of these transitions comes predominantly from mixing of metal $3p$ [68] or $3p$ and $4p$ [54] character with the ligand $2s$ orbitals. Results obtained by Mukoyama *et al.* [71] suggest that most of the strength of the transitions comes from the metal p character of the orbitals, but since a large fraction of the electron density in the initial orbital is on the ligand, Bergmann [23] and de Groot [46] argue that interatomic label for $K\beta''$ still seems appropriate.

In line with the assumption proposed by Bergmann *et al.* [23], the plot of Fig. 7(a) would correspond to the relative $K\beta''$ transition probability per V-ligand pair. Bergmann *et al.* [23] argue that in perturbation theory the amount of metal p and ligand $2s$ mixing will depend on the overlap of these wave functions, and since they have exponential tails, this overlap and hence the observed correlation between $K\beta''$ normalized intensity and average bond length should vary exponentially with distance.

Visual inspection of Fig. 7(b) suggests grouping of data related to $K\beta_{2,5}$ relative intensities around exponential fit for all the measured samples, including oxides, VN, VC, and vanadium metal. $K\beta_{2,5}$ has been assigned to dipole transitions that fill the metal $1s$ vacancy from molecular orbitals with some metal $3d$ and/or $4p$ character along with ligand $2p$ or $3p$ character. Apart from such dipole x-ray emission, there can be some quadrupole x-ray emission directly from the metal $3d$ states [46], which complicates analysis of this x-ray line.

In case of vanadium metal, thick target self-absorption may play an important role in the analysis of $K\beta_{2,5}$ intensity, due to a prepeak in the normalized absorption coefficient (see Fig. 2) whose energy is very close to the energy of the $K\beta_{2,5}$ line. As already explained, in this work we adopted the $K\beta_{2,5}$ x-ray line energy of 5462.96 eV reported by Bearden [28]. Corresponding correction factor due to sample self-absorption of 1.042 results with the relative $K\beta_{2,5}$ intensity of 1.46% reported in Table I. However, energies of $K\beta_{2,5}$ x-ray line reported by some other authors span the range of about 2 eV. For example, one of the possible transition energies extracted from the Sevier's compilation of binding energies [72] is 5464.96 eV, for which the correction due to the sample self-absorption would be 1.6, therefore increasing the relative $K\beta_{2,5}$ intensity (divided with the number of V-ligand bonds) given in Fig. 7(b) from 0.183% to 0.273%.

Results presented at Fig. 7(c) suggest exponential relationship between $(K\beta''+K\beta_{2,5})$ normalized intensities and average bond distances for all the measured vanadium samples, with some deviations for V_2O_3 and VCl_2. V_2O_3 deviation is translated from the same deviation observed for $K\beta''$ x-ray line [Fig. 7(a)], while the deviation related to VCl_2 could be related to the fact that in its spectra $K\beta''$ has not been observed. The result related to VN agrees well with the fit, although corresponding results for $K\beta''$ and $K\beta_{2,5}$ show deviations from the proposed fits. One explanation could be in a possible underestimated $K\beta''$ and overestimated $K\beta_{2,5}$ intensities as determined by fitting of the VN spectra.

Table II shows our results for $K\beta''$ and $K\beta_{2,5}$ energies relative to the $K\beta_{1,3}$ peak energy. Figure 9 shows that the energy difference between $K\beta_{2,5}$ and $K\beta_{1,3}$ increases with the oxidation number in a similar way as in the case of an

other $3d$ transition metal compounds [23]. It was already pointed out by Koster and Mendel [16] and others [23,73,74] that the energy separation between $K\beta_{2,5}$ and $K\beta''$ is approximately given by the energy difference between the ligand $2s$ and $2p$ energy levels, while Bergman *et al.* [23] proposed that this energy difference may be a useful measure to identify the type of ligand in a transition metal compound. Since their proposal was based on only several measured Mn compounds we studied the available literature for reported $K\beta_{2,5}$ and $K\beta''$ energy separations related to transition metal compounds. Table III shows a compilation of available literature data for various Sc, Ti, V, Cr, and Mn compounds with four different ligands (carbon, nitrogen, oxygen, and fluorine). The table shows that $\Delta E(K\beta_{2,5}-K\beta'')$ is a very regular property of the ligand atom. As such it may indeed be used to identify the type of ligand in a number of transition metal compounds.

C. $K\beta'''$ x-ray line

As already mentioned, $K\beta'''$ x-ray line is most probably $K\beta L^1$ satellite that corresponds to the $K\beta_{1,3}$ diagram line, but emitted with one additional L spectator vacancy. The measured energy shift for vanadium sample of 57 eV (Table IV) is close to the value of 63 eV obtained by the Hartree-Fock-Slater (HFS) calculations [75].

According to the measured results given in the Table IV, energy shifts $\Delta E(K\beta'''-K\beta_{1,3})$ are smaller for vanadium compounds then for vanadium metal. It may be seen that for binary oxides, the energy shift increases with the oxidation number, from 50.8 eV for V_2O_3, 51.4 eV for VO_2, to 54.0 eV for V_2O_5. However, such dependence of the energy shift to oxidation number cannot be generalized to all compounds.

From the results related to the $K\beta'''$ relative intensities we could not make a general conclusion on the influence of the oxidation state. It may be seen that for binary oxides, relative intensities increase with the oxidation number.

The results obtained for this x-ray line are strongly influenced by uncertainties in the related absorption coefficients (Fig. 2), and uncertainty of the ratios of cross sections for double ionizations σ_{KL} to single ionization σ_K. This ratio is a function of the projectile energy and is not well known. As explained, in calculating the self-absorption correction factor, we have used an experimentally determined double to single ionization cross sections as reported by Cue *et al.* [45]. As elaborated by Kavčič *et al.* [76], better estimate of this correction factor would require taking in to account the rearrangement processes in the L-shell prior to the x-ray emission. Further measurements on thin targets might help to avoid the above mentioned problems with the analysis of $K\beta'''$ data obtained on thick targets.

ACKNOWLEDGMENTS

Thanks are due to Dr. Ken-Ichi Hasegawa from the Research Center for Ion Beam Technology of the Hosei University, Koganei, Tokyo, Japan, who provided us with the PSPC equipment and WD spectrometer design.

[1] T. Mukoyama and K. Taniguchi, X-Ray Spectrom. **29**, 426 (2000).
[2] M. Polasik, Phys. Rev. A **58**, 1840 (1998).
[3] F. Pawłowski, M. Polasik, S. Raj, H. C. Padhi, and D. K. Basa, Nucl. Instrum. Methods Phys. Res. B **195**, 367 (2002).
[4] S. Raj, H. C. Padhi, and M. Polasik, Nucl. Instrum. Methods Phys. Res. B **145**, 485 (1998).
[5] S. Raj, H. C. Padhi, D. K. Basa, M. Polasik, and F. Pawlowski, Nucl. Instrum. Methods Phys. Res. B **152**, 417 (1999).
[6] S. Raj, H. C. Padhi, M. Polasik, and D. K. Basa, Solid State Commun. **110**, 275 (1999).
[7] H. C. Padhi, C. R. Bhuinya, and B. B. Dhal, J. Phys. B **26**, 4465 (1993).
[8] J. H. Scofield, Phys. Rev. A **9**, 1041 (1974).
[9] A. Perujo, J. A. Maxwell, W. J. Teesdale, and J. L. Campbell, J. Phys. B **20**, 4973 (1987).
[10] T. Mukoyama, Spectrochim. Acta, Part B **59**, 1107 (2004).
[11] A. Servomaa and O. Keski-Rahkonen, J. Phys. C **8**, 4124 (1975).
[12] M. Budnar, A. Mühleisen, M. Hribar, H. Janžekovič, M. Ravnikar, Ž. Šmit, and M. Žitnik, Nucl. Instrum. Methods Phys. Res. B **63**, 377 (1992).
[13] K. Tsutsumi, J. Phys. Soc. Jpn. **14**, 1696 (1959).
[14] K. Tsutsumi, H. Nakamori, and K. Ichikawa, Phys. Rev. B **13**, 929 (1976).
[15] D. Burch, L. Wilets, and W. E. Meyerhof, Phys. Rev. A **9**, 1007 (1974).
[16] A. S. Koster and H. Mendel, J. Phys. Chem. Solids **31**, 2511 (1970).
[17] A. S. Koster and H. Mendel, J. Phys. Chem. Solids **31**, 2523 (1970).
[18] Stuart D. Gamblin and David S. Urch, J. Electron Spectrosc. Relat. Phenom. **113**, 179 (2001).
[19] G. Peng, F. M. F. deGroot, K. Hämäläinen, J. A. Moore, X. Wang, M. M. Grush, J. B. Hastings, D. P. Siddons, W. H. Armstrong, O. C. Mullins, and S. P. Cramer, J. Am. Chem. Soc. **116**, 2914 (1994).
[20] J. T. Armstrong, Anal. Chem. **71**, 2714 (1999).
[21] K. Sakurai and H. Eba, Nucl. Instrum. Methods Phys. Res. B **199**, 391 (2003).
[22] K. Sakurai and H. Eba, J. Solid State Chem. **178**, 370 (2005).
[23] U. Bergmann, C. R. Horne, T. J. Collins, J. M. Workman, and S. P. Cramer, Chem. Phys. Lett. **302**, 119 (1999).
[24] K. Maeda, K. Hasegawa, and K. Ogiwara, Nucl. Instrum. Methods Phys. Res. B **134**, 418 (1998).
[25] L. Mandić, M.Sc. Thesis, University of Zagreb, 2005.
[26] M. Bogovac, I. Bogdanović, S. Fazinić, M. Jakšić, L. Kukec, and W. Wilhelm, Nucl. Instrum. Methods Phys. Res. B **89**, 219 (1994).
[27] J. Végh, Nucl. Instrum. Methods Phys. Res. A **557**, 639

(2006).
[28] J. A. Bearden, Rev. Mod. Phys. **39**, 78 (1967).
[29] W. H. McMaster, N. K. Del Grande, J. H. Mallett, J. H. Hubbell, Compilation of x-ray Cross Sections, Report UCRL-50174, 1969, Lawrence Livermore National Laboratory, Livermore, California, USA.
[30] J. Leroux and T. P. Thinh, *Revised tables of x-ray attenuation coefficients* (Corporation Scientifique Claisse, Quebec, 1977); T. P. Thinh and J. Leroux, X-Ray Spectrom. **8**, 85 (1979).
[31] M. J. Berger and J. H. Hubbell, *XCOM: Photon Cross Sections on a Personal Computer*, NBSIR 87–3597 (1987).
[32] I. Orlić, I. Bogdanović, Shijun Zhou, and J. L. Sanchez, Nucl. Instrum. Methods Phys. Res. B **150**, 40 (1999).
[33] A. Meisel, G. Leonhards, and R. Szargan, *X-ray spectra and chemical binding* (Springer-Verlag, Berlin Heidelberg New York, 1989), Chap. 6.3.2., p. 255.
[34] S. I. Salem, C. N. Chang, and T. J. Nash, Phys. Rev. B **18**, 5168 (1978).
[35] M. Dubiel, S. Brunsch, M. Leister and D. Ehrt, www-hasylab.desy.de/science/annual-reports/1999_report/part1/contrib/42/445.pdf.
[36] J. Wong, F. W. Lytle, R. P. Messmer, and D. H. Maylotte, Phys. Rev. B **30**, 5596 (1984).
[37] I. Orlić, J. Makjanić, G. H. J. Tros, and R. D. Vis, Nucl. Instrum. Methods Phys. Res. B **49**, 166 (1990).
[38] M. Blaauw, J. L. Campbell, S. Fazinić, M. Jakšić, I. Orlić, and P. Van Espen, Nucl. Instrum. Methods Phys. Res. B **189**, 113 (2002).
[39] J. F. Janni, At. Data Nucl. Data Tables **27**, 147 (1982).
[40] W. Brandt and G. Lapicki, Phys. Rev. A **20**, 465 (1979).
[41] W. Brandt and G. Lapicki, Phys. Rev. A **23**, 1717 (1981).
[42] D. D. Cohen and M. Harrigan, At. Data Nucl. Data Tables **33**, 255 (1985).
[43] O. Benka, A. Kropf, At. Data Nucl. Data Tables **22**, 219 (1978).
[44] H. Paul and J. Sacher, At. Data Nucl. Data Tables **42**, 105 (1989).
[45] N. Cue, V. Dutkiewicz, P. Sen, and H. Bakhru, Phys. Lett. **46A**, 151 (1973).
[46] F. deGroot, Chem. Rev. (Washington, D.C.) **101**, 1779 (2001).
[47] M. Uršič, M. Kavčič, and M. Budnar, Nucl. Instrum. Methods Phys. Res. B **211**, 7 (2003).
[48] S. I. Salem, G. M. Hockney, and P. L. Lee, Phys. Rev. A **13**, 330 (1976).
[49] Y. Tamaki, X-Ray Spectrom. **24**, 235 (1995).
[50] B. Ekstig, E. Kallne, E. Noreland, and R. Manne, J. de Physique, J. Phys. (Paris), Colloq. supplement au No 10 Vol. **32**, C4-214 (1971).
[51] M. A. Blokhin and A. T. Shuvaef, Bull. Acad. Sci. USSR, Phys. Ser. (Engl. Transl.) **26**, 429 (1962).
[52] A. T. Shuvaef and G. M. Kulyabin, Bull. Acad. Sci. USSR, Phys. Ser. (Engl. Transl.) **27**, 331 (1963).
[53] E. Asada, T. Takiguchi, and Y. Suzuki, X-Ray Spectrom. **4**, 186 (1975).
[54] J. B. Jones and D. S. Urch, J. Chem. Soc. Dalton Trans., **1975**, 1885.
[55] B. Möser, Cryst. Res. Technol. **20**, 1503 (1985).
[56] T. Mukoyama, K. Taniguchi, and H. Adachi, Phys. Rev. B **34**, 3710 (1986).
[57] R. E. Newnham and Y. M. de Haan, Z. Kristallogr. **117**, 235 (1962).
[58] G. Anderson, Acta Chem. Scand. **10**, 623 (1956).
[59] F. Thesbald, R. Cabala, and J. Bernard, J. Solid State Chem. **17**, 431 (1976).
[60] H. G. Bachmann, F. R. Ahmed, and W. H. Barnes, Z. Kristallogr. Mineral. **115**, 110 (1961).
[61] R. Enjalbert and J. Galy, Acta Crystallogr. **C42**, 1467 (1986).
[62] H. T. Evans, Jr., Z. Kristallogr. Mineral. **114**, 257 (1960).
[63] E. Rudy, F. Benesovsky, and L. Toth, Z. Metallkd. **54**, 345 (1963).
[64] R. W. G. Wyckoff, *Crystal Structures*, 2nd edition (Wiley, New York, 1963), Vol. 1, p. 91.
[65] M. Tachez, F. Théobald, and R. Mercier, Acta Crystallogr. **B35**, 1545 (1979).
[66] I. R. Beattie, M. D. Spicer, and N. A. Young, J. Chem. Phys. **100**, 8700 (1994).
[67] M. Hargitta, O. V. Dorofeeva, and J. Tremmel, Inorg. Chem. **24**, 3963 (1985).
[68] P. E. Best, J. Chem. Phys. **44**, 3248 (1966).
[69] J. Kawai, E. Nakamura, Y. Nihei, K. Fujisawa, and Y. Gohshi, Spectrochim. Acta, Part B **45B**, 463 (1990).
[70] R. J. H. Clark, in *Comprehensive Inorganic Chemistry*, edited by J. C. Bailar, H. J. Emeleus, R. Nyholm, A. F. Trotman-Dickenson (Pergamon, Oxford, 1973), Vol. 3, Chap. 34.
[71] T. Mukoyama, K. Taniguchi, and H. Adachi, Phys. Rev. B **41**, 8118 (1990).
[72] K. D. Sevier, At. Data Nucl. Data Tables **24**, 323 (1979).
[73] V. A. Gubanov, B. G. Kasimov, and E. Z. Kurmaev, J. Phys. Chem. Solids **36**, 861 (1975).
[74] L. M. Sheludchenko, Yu. N. Kucherenko, and V. G. Aleshin, J. Phys. Chem. Solids **42**, 733 (1981).
[75] D. Burch, L. Wilets, and W. E. Meyerhof, Phys. Rev. A **9**, 1007 (1974).
[76] M. Kavčič, M. Budnar, and J. L. Campbell, Nucl. Instrum. Methods Phys. Res. B **196**, 16 (2002).
[77] I. Török, T. Papp, J. Pálinkás, M. Budnar, A. Mühleisen, J. Kawai, and J. L. Campbell, Nucl. Instrum. Methods Phys. Res. B **114**, 9 (1996).
[78] L. Ramquist and R. Manne, J. Phys. Chem. Solids **32**, 149 (1971).
[79] M. Romand and J. S. Solomon, Spectrochim. Acta, Part B **28B**, 17 (1973).
[80] M. A. Blokhin and A. T. Shuaev, Bull. Acad. Sci. USSR, Phys. Ser. (Engl. Transl.) **26**, 429 (1962).
[81] E. E. Vainshtein and V. I. Chirkov, Sov. Phys. Dokl. **7**, 724 (1963) [Dokl. Akad. Nauk SSSR **145**, 1031 (1962)]; E. A. Shurakovskii and E. E. Vainshtein, *ibid.* **4**, 1308 (1960) [Dokl. Akad. Nauk SSSR **129**, 1269 (1959)].
[82] V. Ern and A. C. Switendick, Phys. Rev. **137**, A1927 (1965).
[83] G. Dräger, O. Brümmer, V. Heera, G. Seifert, and P. Ziesche, Phys. Status Solidi B **104**, 219 (1981).